Characterization of dermal structural assembly in normal and pathological connective tissues by intrinsic signal multiphoton optical microscopy

Julia G. Lyubovitsky[a]*, Xiaoman Xu,[b] Chung-ho Sun,[c] Bogi Andersen,[b] Tatiana B. Krasieva[c] and Bruce J. Tromberg[c,d]

[a]Bioengineering Department, University of California, Riverside, CA 92521
[b]Medicine (Endocrinology) and Biological Chemistry Departments,
University of California, Irvine, CA USA
[c]Laser Microbeam and Medical Program, Beckman Laser Institute,
University of California, Irvine, CA USA
[d]Biomedical Engineering Department, University of California, Irvine, CA USA

ABSTRACT

Employing a reflectance multi-photon microscopy (MPM) technique, we developed novel method to quantitatively study the three-dimensional assembly of structural proteins within bulk of dermal ECMs. Using a structurally simplified model of skin with enzymatically dissected epidermis, we find that low resolution MPM clearly discriminates between normal and pathological dermis. High-resolution images revealed that the backscattered MPM signals are affected by the assembly of collagen fibrils and fibers within this system. Exposure of tissues to high concentrations of potentially denaturing chemicals also resulted in the reduction of SHG signals from structural proteins which coincided with the appearance of aggregated fluorescent structures.

Keywords: bioimaging; multiphoton microscopy; second harmonic generation; two-photon fluorescence; dermis; collagen, remodeling; disassembly; aminogunidine; urea

1. INTRODUCTION

Biomedical imaging using multiphoton microscopy (MPM) combines backscattered second harmonic generation (SHG) and two-photon fluorescence (TPF) intrinsic signals. Transgenic mouse model of Clim transcriptional co-activators of LIM domain proteins[1] has facilitated the establishment of the sensitivity and value of these signals in detecting extracellular matrix (ECM) changes in several connective tissues due to gene alterations.[2-4] The dominant negative Clim is expressed under the K14 promoter in the epithelial tissues of mice and is involved in organ development and cancer. The transgenic animals progressively develop corneal abnormalities, pathological hair cycling that results in a hair loss and some mice acquire chronic wounds on the upper parts of their back. This mouse model[1] was originally created to test the role of Clim genes in the development of stratified epithelial tissues.

*Contact julial@ucr.edu; phone 951-827-7231; fax 951-827-6416; Bioengineering Department, 900 University Avenue, Riverside, CA 92521.

It expresses the transgene in the basal cell layer of the epidermis, the outer root sheath of hair follicles, the basal cell layer of neonatal corneal epithelium, and limbal cells of adult corneal epithelium.

In this paper, we report an MPM-based approach that combines backscattered intrinsic second harmonic generation (SHG) and two-photon fluorescence (TPF) signals to detect structural changes of the dermal collagen proteins within the skin organ. The overarching goal is to extend the applications of MPM-based techniques to understanding the mechanism of supramolecular assembly of structural proteins within connective tissues and other natural bio-composites.

2. METHODS

Multiphoton microscopy (MPM) imaging: The non-descanned inverted muliphoton laser scanning microscope used is described elsewhere (Ref. [3,5,6] and references therein). The samples were imaged under standard thickness coverglass using 10X air (NA = 0.33) and 40X water (NA = 0.8) for quantitative work and 63X water (NA = 1.2) for high resolution imaging. The laser excitation was linearly polarized at 800 nm and verified with a BBO nonlinear crystal placed on the microscope stage. Day to day uncertainties in measuring fluorescence and SHG intensities were established with fluorescein solutions and SHG nonlinear crystals (z-cut quartz and others). Spectral filtering with dichroic (500 nm) and a bandpass filter (400AF10 for λ_{ex} = 800 nm) was used to separate the second harmonic signal of ECM from that of intrinsic fluorescence. The autofluorescence was further separated into blue (using 445$\pm$25 nm filter) and red (using 520$\pm$30 nm filter or 580$\pm$30 nm filter) components. Depth dependence curves of backscattered SHG intensity from dermis were acquired by moving the objective from the surface of the coverglass into the samples using computer controlled LUDL MAC2000 stage controller equipped with a stepper motor. At different laser focus depth there was a different value of SHG intensity integrated over the entire image area. As the laser focus was moved deeper into the tissue, the SHG intensity first built up and then decayed due to both attenuation of excitation and attenuation of scattered signal. Given the complexity in the relationship between laser-tissue interaction and signals detected, to quantify the latter, we integrated the areas under the depth dependence curves of backscattered SHG intensity from baseline.

Tissue samples: All animal procedures were performed in accordance with an animal protocol approved by the University of California at Irvine. Mice strain CB6F1 was used in all experiments. Clim transgenic mice were generated as described in Ref. [1]. The transgenic mice exhibited corneal and skin abnormalities in addition to pathological hair cycling and differentiation. Immediately after euthanasia by asphyxiation with CO_2, the animals were shaved and subjected to 4 min treatment with Nair (Ralphs) to remove residual hair. The skins were surgically removed from the backs of the animals and thoroughly rinsed three times with PBS solution that contained antibiotics gentamicin sulfate (Fisher Scientific) at 200ug/ml (4x of the normal working concentration) and amphotericin B (SigmaAldrich) at 22.4ug/ml (4x of the normal working concentration). The tissues were cut into smaller pieces and treated with dispase for two hours at 37°C to remove epidermis. After rinsing skins with 0.9% saline solution they were immediately imaged with an inverted two-photon microscope. Three dimensional reconstructions of dermis up to 100 μm into the tissues were collected in under five minutes utilizing native signals only. The ages of mice imaged were 5 months to about one year.

***In situ* chemical remodeling of dermis:** 8 M urea (Sigma), 2 M glucose (Sigma), 2 M sorbitol (Sigma) and 0.25 M aminoguanidine (Sigma) solutions were prepared in potassium phosphate buffer (KPi, pH 7.2, μ 0.1 M) and their pH was adjusted to 7.1-7.3 using concentrated aqueous NaOH and HCl. For equilibrium dermis denaturation experiments, freshly excised skin samples (5 mm x 5mm) with enzymatically removed dermis were added to 5 mL pH-adjusted (pH 7.3) solutions. Samples were then equilibrated at room temperature overnight with continuous shaking prior to imaging. For dynamic denaturation experiments, 5-8 drops of denaturing solution were added from above to the area of the field of view. Images within the same optical section were recorded as a function of time after application.

3. RESULTS AND DISCUSSION

To test the capability of multiphoton microscopy to quantitatively evaluate structural changes within dermal collagen upon a selected perturbation, we gently separated epidermis from dermis using dispase. A brief treatment with dispase cleaves collagen type IV of the basement membrane that links epidermis and dermis without affecting underlying structures of collagen type I fibers. This gentle enzymatic processing of tissue samples allowed acquisition of high contrast three dimensional optical slices of the collagen fiber network inside dermis within minutes.

3.1 Normal dermis studied with intrinsic signal MPM

To evaluate the structural fiber arrangement and form within normal dermis using MPM optical tomography, we initially mapped its three dimensional organization at different magnifications. At least two clearly structurally distinct layers were observed at high resolution utilizing SHG signals only (Figure 1). Based on earlier electron microscopy work, the layers imaged were recognized as papillary and reticular. Both experimentally collected *en face* and reconstructed transverse optical sections (not shown) were rapidly obtained. They were used to examine collagen fibers within observed dermal layers. The fibers did appear to have elliptical cross-sections. The upper, papillary layer that the epidermis rests on (Figure 1B) contained an arrangement of thin fibers with an average major axis of 2 to 3 μm. The lower, reticular layer (Figure 1C) was made of thick collagen fiber bundles preferentially oriented parallel to the surface of the skin with an average major axis of 6.3 μm in a 5 months old animal. At these high magnifications the fibrillar composition of many fibers could be distinguished with most fibrils aligned parallel to the length of the fiber (Figure 1B). The part of dermis that did not generate SHG signal and appeared as a dark area between fibers is denoted by a star.
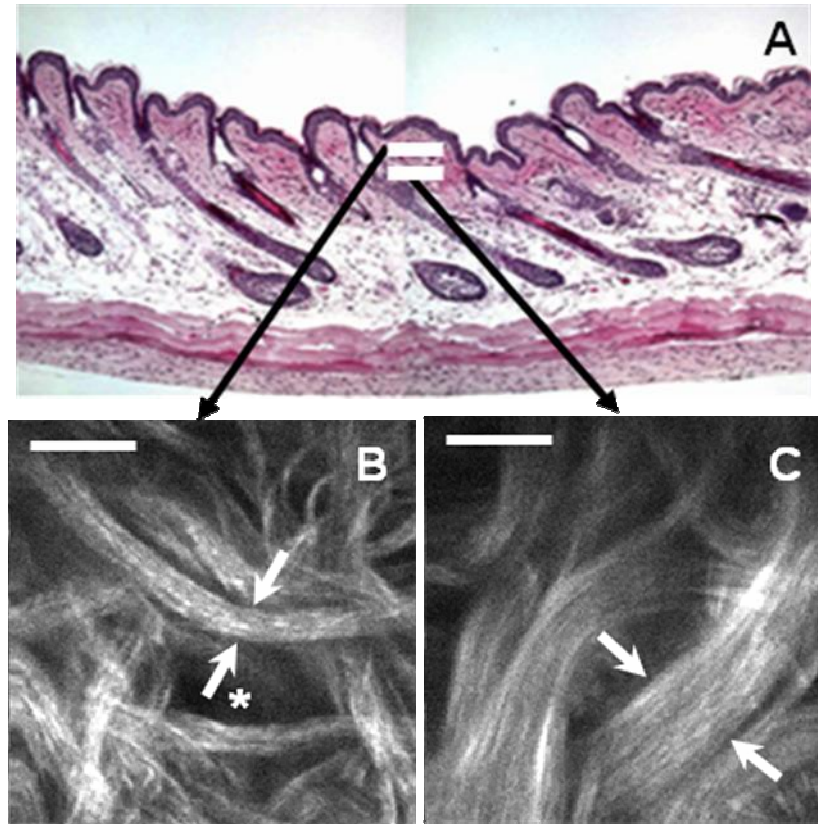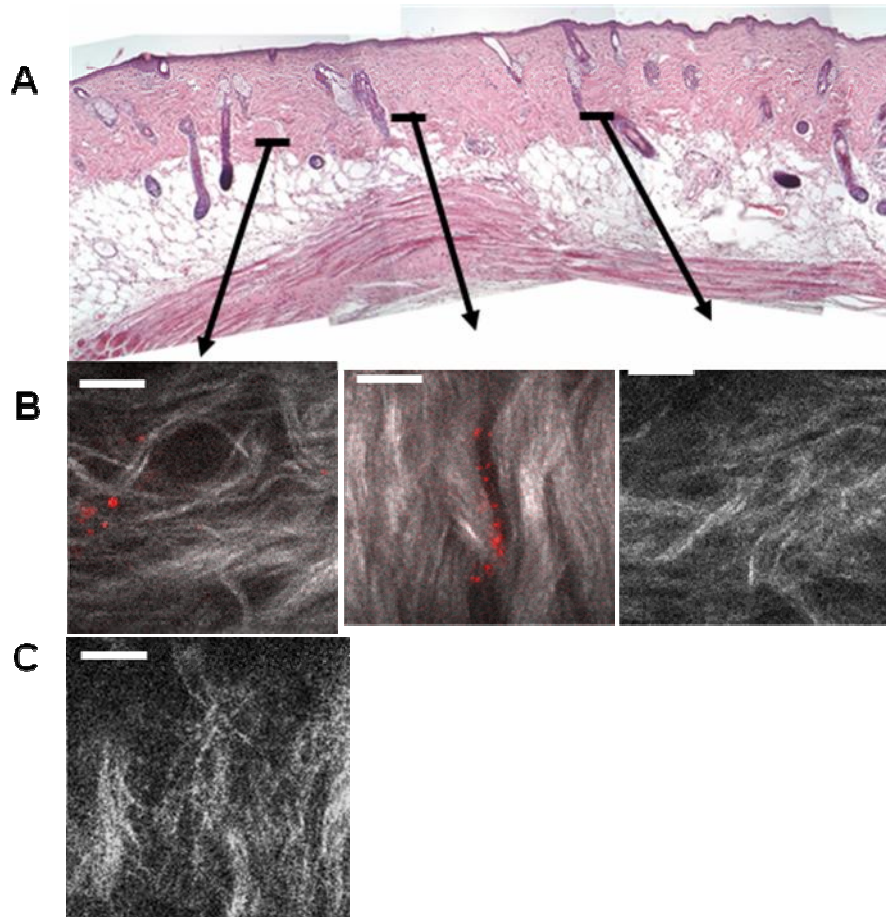
Figure 1. (A) Reconstruction of a transverse histological section through the normal mouse skin. (B) Typical *en face* high resolution MPM optical section through a papillary collagen layer 8 μm deep inside dermal connective tissue. Scale bar is 10 μm. (C) Typical *en face* high resolution MPM optical section through a reticular collagen layer observed 24 μm deep inside dermal connective tissue. Scale bar is 10 μm.

The structural features of normal dermis surrounding hair follicle structures were also investigated in detail. High magnification *en-face* MPM optical sections [4] showed finger-like protrusions of ECM filled with material that did not appear to form fibrils resolvable by optical imaging in a backscattering configuration.

3.2 Pathological changes in K14-DN-Clim mice dermis detected with intrinsic signal MPM

Upon establishing the origins of SHG forming signals within normal dermal connective tissues, we examined the structure of ECM in a mild and terminal phenotype transgenic mouse model of a Clim[7-12] transcriptional factor involved in organ development and cancer. In the mild transgenic mouse phenotype, high resolution SHG images revealed dermis structured similar to normal. In the terminal phenotype, dermis was highly remodeled with no distinct papillary or reticular layers throughout its thickness (Figure 2B). Instead of collagen fiber bundles observed in the normal dermal connective tissues, collagen fiber network appeared significantly compromised and presented as a highly disorganized collection of thin SHG generating threads and punctate areas. Red autofluorescence collected with 580±30 μm filter was co-localized with the most profound alterations in the ECM (Figure 2B). It was detected 24 μm and deeper inside freshly excised tissues

(under 2 hours after sacrificing the animals) that were extensively rinsed with an antibiotic solution prior to removal of epidermis and therefore, cannot be attributed to postmortem infestations. Upon visual inspection, animals that presented terminal phenotype imaged in Figure 2B were completely bald with hair remaining only on the head and parts of neck area. The skin had sores over entire animals' body. It looked raw and did not have a typical lustrous look. The blood vessels with overgrown inclusions were observed inside dermal tissue throughout the animal. A typical histological observation of skin in Clim terminal phenotype (Figure 2A), reveled a thicker

Figure 2. (A) Reconstruction of a transverse histological section through the terminal phenotype transgenic mouse skin ([1]); (B) Typical *en face* high resolution MPM optical sections through various depths inside Figure 2A; (C) Nonspecific infestation of tissues left in 50 mM phosphate buffer for 48 hrs. Scale bar is 8 μm.

looking compared to normal dermis. Due to inability to resolve structural features of collagen fiber network within ECM with this technique, the nature of thickening could not be uncovered from a routine histology. The nonspecific infestation of tissues left in 50 mM phosphate buffer for 48 hr produced SHG signals structurally reminiscent of those observed in terminal phenotype transgenic dermis (Figure 2C).

A significant loss of thick assembled collagen fiber bundles inside dermis of terminal phenotype transgenic mouse model was quantified using the area under the depth dependence curve of

backscattered SHG intensity collected to the depth of about 90 μm. The area under the depth dependence curve of backscattered SHG intensity for the terminal Clim mouse phenotype was about 90% smaller compared to that collected from normal dermis (Figure 3). For the mild transgenic mouse phenotype that as judged from MPM images had dermis assembled similar to normal, the difference was not as pronounced and accounted for about 13%.
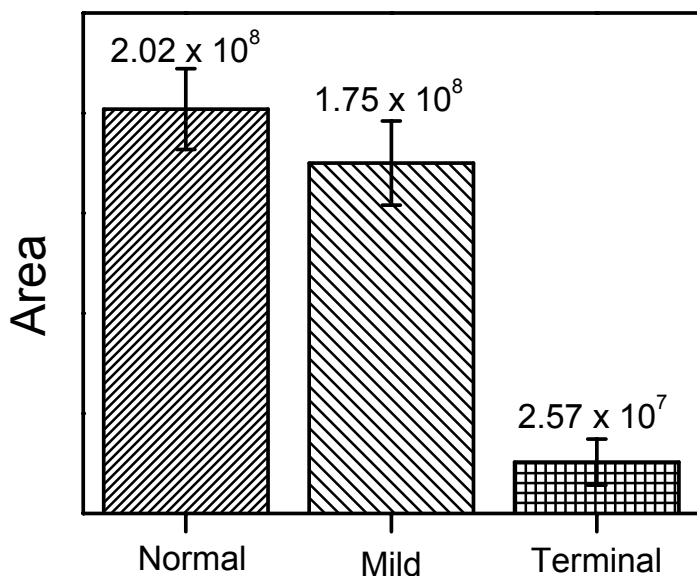

Figure 3. The difference in scattering was quantified utilizing the integrated areas under the depth dependence curves of backscattered SHG intensity collected to the depth of about 90 μm. The total volume of dermal tissue sampled was 324E+3 μm^3.

Preliminary investigations of dermal ECM arrangement and form in the pathological hair follicles showed that these were also modified compared to normal follicular structures.[4]

3.3 Chemical remodeling of normal dermis studied with intrinsic signal MPM

To understand the role of the assembly of collagen in generation of intrinsic MPM signals, we perturbed is with high concentrations of urea, aminoguanidine and other chemicals (see METHODS section) that could potentially disassemble collagen molecular and supramolecular structures. The kinetics of collagen remodeling was followed utilizing backscattered SHG signal intensity inside the dermal connective tissue (Figure 3). The progressive loss of SHG signal from collagen fibers upon destabilizing protein structure within ECM with aminoguanidine (Figure 3A) coincided with the appearance of 'clumped' species within the 'holes' generated upon remodeling/denaturation at later times. The fluorescence of these species was detected with a 520±30 nm filter. Fluorescent

'clumped' structures were observed during dynamic denaturation of dermal connective tissues with urea and previously in tissue engineered systems incubated with 0.6 M glucose.[13]
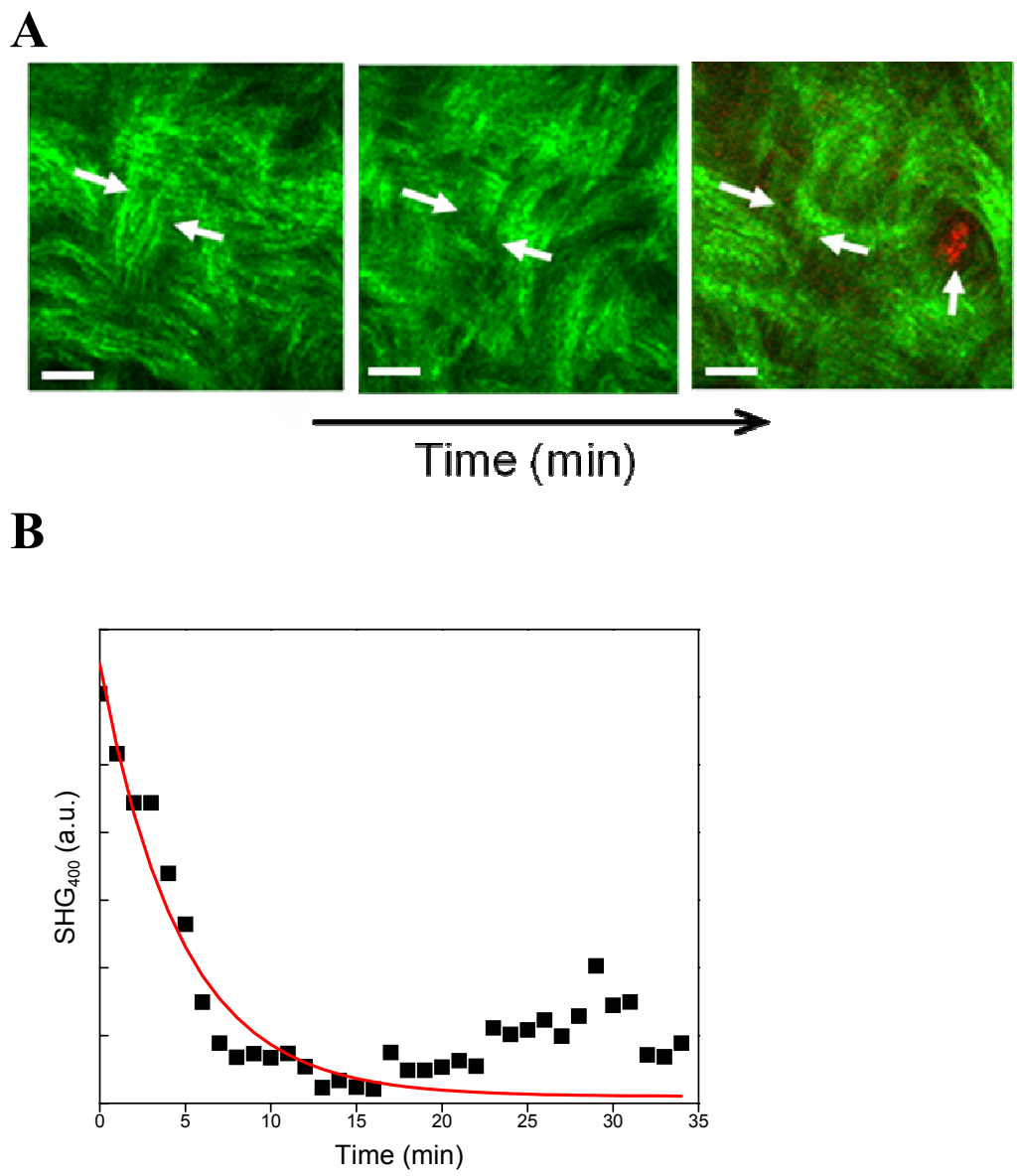
A

B

Figure 3. Kinetics of *in-situ* chemical remodeling within normal mice dermis detected and quantified using MPM signals. (A) SHG (green pseudocolor) detected with 400AF10 filter is generated by collagen fiber bundles within dermis. The progressive remodeling of ECM upon destabilizing protein structures with 8 M urea, 2 M glucose, 2 M sorbitol and 0.25 M aminoguanidine is accompanied by appearance of 'clumped' species at later times within generated 'holes'. The fluorescence (red pseudocolor) of these species was detected with a 520 ± 30 nm filter. Note arrows denoting progressive disappearance of a group of SHG generating collagen fibers in the middle of the image and appearance of fluorescent 'clumped' structures within a void generated on the right. The images were collected at times 2 min, 10 min and 25 min after application of a particular chemical. (B) A typical kinetic trace showing the effect of destabilizing chemicals

on collagen fiber structures within dermis monitored by following SHG signal intensity with a 400AF10 filter. To guide the eye, the data points were fit to a single exponential (red line). Scale bar is 10 μm.

In spite of the fact that total loss in SHG intensity and restructuring of collagen fibers within dermis was detected in MPM images for all chemicals utilized at high concentration, structurally collagen fibers appeared different from those observed in the terminal phenotype dermal tissues. Only nonspecific infestation of tissues left in 50 mM phosphate buffer for 48 hr produced SHG signals (Figure 2C) structurally reminiscent of those observed in terminal phenotype transgenic dermis (Figure 2B, right). Based on these observations, we suggest that at least in part, loss of SHG signal inside dermis detected in the terminal phenotype of transgenic mice is due to remodeling of connective tissues by proteases present during inflammatory processes induced in the animals by genetic changes (B. Andersen, unpublished data and Ref. 1).

4. CONCLUSION

The assembly of structural proteins within ECM can be easily disrupted by genetic, chemical and physical perturbations leading to proteolysis, nonspecific aggregation and cross-linking. In this work we show that high-resolution MPM optical tomography measurements on dermal connective tissues reveal a large degree of such destabilization in the terminal phenotype of a genetically altered dermis. We quantified this alteration by integrating the area under a depth dependence curve of reflected SHG intensity. To understand the changes within collagen at the molecular level, we modulated the properties of ECM structural proteins. Our work shows how this technology could soon become an indispensable tool to non-destructively monitor and arrest dermal inflammatory processes resulting in proteolytic degradation of ECM proteins that lead to destabilized structures within connective tissues, abnormal wound healing and scarring.[14] It can be used to understand the mechanisms of collagen fibrillogenesis and remodeling in any connective[2,3] or bioengineered tissue.[15]

ACKNOLEGEMENTS

REFERENCES

(1)   Xu, X.; Mannik, J.; Kudryavtseva, E.; Lin, K. K.; Flanagan, L. A.; Spencer, J.; Soto, A.; Wang, N.; Lu, Z.; Yu, Z.; Monuki, E. S.; Andersen, B., "Co-factors of LIM domains (Clim/Ldb/Nli) regulate corneal homeostasis and maintenance of hair follicle stem cells", *Developmental Biology* **2007**, *312*, 484-500.

(2)   Lyubovitsky, J. G.; Krasieva, T. B.; Spencer, J. A.; Andersen, B.; Tromberg, B. J.,"Corneal damage revealed by endogenous cellular fluorescence", *Proc. SPIE* **2005**, *5700*, 213-217.

(3)   Lyubovitsky, J. G.; Krasieva, T. B.; Spencer, J. A.; Andersen, B.; Tromberg, B. J. *J. Biomed. Optics* **2005**, *11*, 014013

(4)   Lyubovitsky, J. G.; Krasieva, T. B.; Xu, X.; Andersen, B.; Tromberg, B. J., "Imaging corneal pathology in a transgenic mouse model using nonlinear microscopy", *J. Biomed. Optics* **2007**, *12*, 044003.

(5)   LaMorte, V. J.; Zoumi, A.; Tromberg, B. J., "Spectroscopic approach for monitoring two-photon excited fluorescence resonance energy transfer from homodimers at the subcellular level", *J. Biomed. Optics* **2003**, *8*, 357-361.

(6)   Zoumi, A.; Yeh, A.; Tromberg, B. J., "Imaging cells and extracellular matrix in vivo by using second-harmonic generation and two-photon excited fluorescence", *Proc. Natl. Acad. Sci. USA* **2002**, *99*, 11014-11019.

(7)   Agulnick, A. D.; Taira, M.; Breen, J. J.; Tanaka, T.; Dawid, I. B.; Westphal, H., "Interactions of the LIM-domain-binding factor Ldb1 with LIM homeodomain proteins", *Nature* **1996**, *384*, 270-272.

(8)   Bach, I.; Carriere, C.; Ostendorff H.P.; Andersen B; M.G., R., "A family of LIM domain-associated cofactors confer transcriptional synergism between LIM and Otx homeodomain proteins", *Genes Dev* **1997**, *11*, 1370-1380.

(9)   Jurata, L. W.; Kenny, D. A.; Gill, G. N., "Nuclear LIM interactor, a rhombotin and LIM homeodomain interacting protein, is expressed early in neuronal development*", Proc Natl Acad Sci U S A* **1996**, *93*, 11693-11698.

(10)   Sugihara, T. M.; Bach, I.; Kioussi C; Rosenfeld MG; B, A.,"Mouse deformed epidermal autoregulatory factor 1 recruits a LIM domain factor, LMO-4, and CLIM coregulators*", Proc Natl Acad Sci U S A* **1998**, *95*, 15418-15423.

(11)   Torigoi, E.; Bennani-Baiti, I. M.; Rosen, C.; Gonzalez, K.; Morcillo, P.; Ptashne, M.; D., D.," Chip interacts with diverse homeodomain proteins and potentiates bicoid activity in vivo", *Proc Natl Acad Sci U S A* **2000**, *97*, 2686-2691.

(12)   Visvader, J. E.; Mao, X.; Fujiwara, Y.; Hahm, K.; Orkin, S. H.,"The LIM-domain binding protein Ldb1 and its partner LMO2 act as negative regulators of erythroid differentiation", *Proc Natl Acad Sci U S A* **1997**, *94*, 13707-13712.

(13)   Zoumi, A., Thesis in Biomedical Engineering, University of California at Irvine, 2003.

(14)   Meshkinpour, A.; Ghasri, P.; Pope, K.; Lyubovitsky, J. G.; Risteli, J.; Krasieva, T. B.; Kelly, K. M.," Treatment of hypertrophic scars and keloids with a radiofrequency device: A study of collagen effects", *Lasers in Surgery a nd Medicine* **2005**, *37*, 343-349.

(15)   Raub, C. B.; Suresh, V.; Krasieva, T.; Lyubovitsky, J.; Mih, J. D.; Putnam, A. J.; Tromberg, B. J.; George, S. C., "Non-invasive assessment of collagen hydrogel microstructure and mechanics using multiphoton microscopy", *Biophys. J.* **2006**, *92* 2212-2222